

CERN-TH-7389/94  
August 1994

# WHITHER DO THE MICROLENSING BROWN-DWARFS ROVE?

A. De Rújula, G. F. Giudice, S. Mollerach and E. Roulet

CERN,  
1211 Geneva 23  
Switzerland

## ABSTRACT

The EROS and MACHO collaborations have reported observations of light curves of stars in the Large Magellanic Cloud that are compatible with gravitational microlensing by intervening massive objects, presumably Brown-Dwarf stars. The OGLE and MACHO teams have also seen similar events in the direction of the galactic Bulge. Current data are insufficient to decide whether the Brown-Dwarfs are dark-matter constituents of the non-luminous galactic Halo, or belong to a more conventional population, such as that of faint stars in the galactic Spheroid, in its Thin or Thick Disks, or in their possible LMC counterparts. We discuss in detail how further observations of microlensing rates, and of the moments of the distribution of event durations, can help resolve the issue of the Brown-Dwarf location, and eventually provide information on the mass function of the dark objects.

CERN-TH.6272/91

August 1994

# 1 Introduction

In a paper uneagerly published in 1936, Einstein (1936) described how the apparent luminosity of a star may be temporarily amplified by the gravitational field of a second star that crosses close to the line of sight to the first. He concluded that the effect was of no practical interest. Half a century later, Paczyński (1986) revised Einstein’s conclusion by noting that the search for microlensing events in the direction of the *Large Magellanic Cloud* (LMC) may resolve the question of the extent to which the mass of the dark Halo of our galaxy is due to *Brown-Dwarfs*, stars too faint to be readily observed otherwise.

The EROS (Aubourg *et al.* 1993) and MACHO (Alcock *et al.* 1993) collaborations have reported “microlensing” events of the expected characteristics in the direction of the LMC, and the MACHO (Alcock *et al.* 1994) and OGLE (Udalski *et al.* 1994) groups have seen similar events in the direction of the “*Galactic Bulge*”, centrally located in the Milky Way. In spite of the currently low statistics, the observers have established that the temporal shape, achromaticity, location in the Hertzsprung-Russell diagram, and non-repetitive character of the events place them far away from the tails of the distributions inferred from the observed variable stars. The events are either due to a novel and most implausible type of variable, whose properties are “just so” as to fool the observer, or to microlensing by the faint interlopers that one is searching for.

We are primarily interested in Brown-Dwarfs, *compact objects* that act as gravitational lenses but that may otherwise be directly observable, with considerable toil, only at infrared wavelengths (Kerins & Carr 1994). Not to shine at visible frequencies, Brown-Dwarfs must be **lighter** than the thermonuclear ignition threshold, which for a compact object predominantly made of H and He is  $m_{max} \sim 0.085M_{\odot}$  (Graboske & Grossman 1971). Not to have evaporated during the age of the Galaxy, these bodies must be **heavier** than  $(10^{-6}-10^{-7})M_{\odot}$  (De Rújula, Jetzer and Massó 1992).

There is a cutoff on the mass of Brown-Dwarfs more stringent than the evaporation limit: the “*Jeans*” mass  $m_{min} \sim 7 \times 10^{-3}M_{\odot}$  (Low & Lynden-Bell 1976), the lowest mass of a detached H/He gas-cloud fragment whose self-gravitational collapse into a compact object is not prevented by the de-

veloping thermal pressure. Although the Jeans limit is not absolute (Jupiter, Saturn, Uranus and Neptune are counterexamples to it), the relatively long durations of the observed microlensing events indicate that the objects responsible for them are in the upper domain of allowed masses, the question of a precise lowest-mass cutoff appears to be rather moot. We shall consequently restrict our considerations to compact objects whose masses range from the Jeans mass to the hydrogen-burning threshold. On-going observations are sensitive to microlensing by objects with masses lying anywhere in this mass range.

The existence of a dark halo in spiral galaxies is decisively demonstrated by their observed rotation curves. The nature of the constituents of this dark mass, contrary-wise, is debatable and debated. An important role in the discussion is played by constraints on the universal average “baryonic” density, stemming from the relative abundances of primordial elements that are inferred, after significant corrections, from spectral observations (Walker *et al.* 1991). Recent measurements of the  $^2\text{H}$  abundance in distant intergalactic clouds (Songaila *et al.* 1994, Carswell *et al.* 1994) favour the conclusion that most baryonic matter is visible and accounted for, leaving no room for a predominantly (baryonic) Brown-Dwarf constituency of our Halo.

Often used as an argument against a Halo made of Brown-Dwarfs is the contention that the density of all other stellar distributions falls off with distance from the galactic centres significantly faster than  $\sim r^{-2}$ , the behaviour required to explain a flat rotation curve. But Sackett *et al.* (1994) have recently observed that the Halo of the spiral NGC5907, though very dim, has a luminosity distribution that traces its dark mass.

In our opinion, it is too early to accept as conclusive the arguments favouring a baryonic or non-baryonic composition of galactic halos. We discuss the direct search for Brown-Dwarfs in the Halo of the Galaxy, if only because failure to find them in significant amounts would constitute the most intriguing observational result: it would strongly advocate for a Halo consisting of a substance more subtle than the ones we are made of.

The interest of Brown-Dwarfs would transcend stellar physics, should they significantly contribute to the Halo dark mass. Thus the spirit in which we shall discuss the microlensing data: Brown-Dwarfs in the Galaxy’s Halo will be considered the “signal”, dim lensing bodies from other stellar populations

will be regarded as “backgrounds”.

Various locations for these backgrounds have been discussed: the *Thin Disk*, the *Thick Disk* (Gould, Miralda-Escudé & Bahcall 1994) and the *Spheroid* (Giudice, Mollerach & Roulet 1994), all of them stellar populations extending beyond the location of our own solar system. Though we are immersed in these stellar distributions, the contribution of their unseen astral bodies to microlensing in the direction of the Magellanic Clouds was once thought to be quite negligible, relative to the full signal of a Brown-Dwarf-dominated Halo. But, if the dark constituency of these galactic components is sizable, they may significantly contribute to the LMC and SMC lensing rates. They could even account for the observations (Gould, Miralda-Escudé & Bahcall 1994, Giudice, Mollerach & Roulet 1994) that, within very poor statistics, seem to fall short of the expected Halo rates. Dim objects in the LMC itself may also contribute to the microlensing of LMC stars.

To visualize the invisible, we show in Fig. 1 contour plots of the different galactic dark-mass distributions that we shall discuss. The  $x$  and  $y$  axis are in the galactic plane, the  $y$  axis digs into the figure. For each population, the inner and outer contours correspond to volume densities of  $10^{-2}M_{\odot}/\text{pc}^3$  and  $10^{-3}M_{\odot}/\text{pc}^3$ . The solar position is at  $(-8.5, 0, 0)$  kpc. The densest and most convenient microlensing target-fields of source stars are the Magellanic Clouds and the galactic Bulge. The LMC, assessing its distance from us to be 55 kpc, is at  $(0, -46, -29)$  kpc. The SMC, reckoned to be located at 65 kpc, is at  $(17, -39, -45)$  kpc. The galactic Bulge fills the central 1–2 kpc. We devote Section 2 to a detailed discussion of the spatial distributions of visible and dark mass in our Galaxy and in the LMC.

In this paper we discuss simple strategies to analyse microlensing data of modest statistics. We combine the modelling of various signal and background stellar populations with the information reflected in the first few moments (De Rújula, Jetzer & Massó 1991) of the event-duration distribution: the number of events (the “zeroth” moment); the average duration  $\langle T \rangle$ ; and the time dispersion  $\Delta T/T \equiv \sqrt{\langle T^2 \rangle - \langle T \rangle^2} / \langle T \rangle$ . The mass function of the lenses (number of objects per unit mass interval) is unknown apriori, and the predictions for the various duration moments depend on its assumed functional form. We deal with this problem by “sweeping” our results over the very large domain of mass-function ansatzes discussed in Section 3.

In Section 4 we recall the basic expressions for the microlensing rate as a function of event duration, in the divers viewing directions of interest, and for the various lensing populations. In Section 5 we develop a feeling for the results by discussing ideal observations of single-mass lensing objects. In Section 6 we discuss realistic limited-statistics observations of objects whose mass function and location are unknown. We illustrate the effects of the detection efficiency as a function of event duration. This is not always possible, since only OGLE has already published the relevant information and MACHO is currently analysing the problem in detail<sup>1</sup>.

The microlensing predictions corresponding to the Halo signal and the various possible backgrounds can be conveniently visualized by plotting the event rate and the event time-dispersion against the mean event duration. For observations in the direction of the Magellanic Clouds, even after the “blurring” induced by the apriori ignorance of the lensing-objects’ mass function, the signal and backgrounds occupy distinct regions of these plots. It is therefore quite conceivable that, as the statistics improves to a few dozen events, the data favour one of these regions and the culprit microlensing star population can be pinned down. This is our main result, which will be reflected in Figs. 4 and 5. The comparison of SMC and LMC observations would also help locating the lensing agents.

In the direction of the Bulge the microlensing observables predicted for the different dark populations overlap to some extent, once the ignorance of the lensing mass function is duly taken into account. Thus, our proposed procedure to select the stellar distribution to which the microlensing objects belong should work for the LMC, but not for the Bulge. There the situation is even more challenging for, as is almost always the case in astronomy, the observations have spoiled the simplicity of the original picture.

The Bulge event rates reported by the OGLE and MACHO collaborations are larger than expected in any simple Brown-Dwarf scenario. And the event durations are surprisingly long. The observed rate can be brought to agree with theory by combining the contributions of several stellar populations. But the rate and the event durations cannot be simultaneously described by any combination of the conventional Halo, Disk and Spheroid dark-matter models (plus the contribution of faint Disk stars). To quantify

---

<sup>1</sup> We are indebted to Pierre Barette for discussions on the EROS efficiencies.

the severity of this problem, and given the scarcity of the data, we must resort to a Kolmogorov–Smirnov test of the time distribution. We conclude that the disagreements are serious enough to justify modifications of the accepted models of the inner galactic realm. Our analysis and some of these modifications (Alcock *et al.* 1994, Paczyński *et al.* 1994) are specified in Section 6d.

The titles and subtitles of Sections 2–6 image the organization of the paper. In the conclusions of Section 7 we fail to be truly conclusive, for our current understanding of galaxies is still modest, and the microlensing observations are still infants.

## 2 Galactic components

In this Section we summarize the hypothesis and empirical constraints concerning the dark mass of the Galaxy and of the Magellanic Clouds.

### *a) The galactic Halo*

We assume the density-profile of our galactic Halo to be spherical<sup>2</sup> and to correspond to a rotation curve flattening at  $v_H \simeq 220$  km/s. Let  $R_\otimes \simeq 8.5$  kpc be our distance to the galactic centre and  $a \sim 3$  kpc the Halo’s “core radius”. We adopt a halo density distribution:

$$\rho(r) = \rho_H \frac{R_\otimes^2 + a^2}{r^2 + a^2}. \quad (1)$$

The uncertainty in  $a$ , which is rather large (Caldwell & Ostriker 1981 and Bahcall, Schmidt & Soneira 1983), significantly affects the microlensing predictions in the direction of the Bulge, but is ineffectual in the direction of the Magellanic Clouds. The rotation curve of our galaxy is only measured out to  $r \sim 20$  kpc (Fich and Tremaine, 1991), and microlensing in the LMC and SMC significantly depends on the assumed Halo density at larger values of  $r$ : it is not possible to assign an empirical error to the predictions for Halo microlensing rates.

---

<sup>2</sup> A flattening of the Halo would be of little relevance to LMC observations, but would increase the optical depth towards the SMC by up to 40% (Sackett & Gould, 1993). The effect of tilting the axis of a non-spherical Halo has been discussed by Frieman & Scoccimarro (1994).

The local halo density implied by fits to the Galaxy’s rotation curve is  $\rho_H \sim 10^{-2} M_\odot/\text{pc}^3$ . If and when a signal for microlensing by objects in our Halo is established, the main result of the observational campaigns would be the comparison of the dynamically-determined value of the dark-mass density with that extracted from the microlensing data. The ratio of this two independent measurements is the fractional contribution of compact objects to the Halo’s dark mass.

The velocities of the constituents of a gravitationally self-consistent spherical Halo are isotropic at any point, and follow a Maxwellian distribution (Chandrasekhar 1942):

$$f(v) = \frac{1}{(2\pi)^{3/2} \sigma^3} e^{-v^2/2\sigma^2} , \quad (2)$$

with a dispersion  $\sigma = v_H/\sqrt{2}$ .

The galactic Halo is overwhelmingly “dark”.

#### *b) The Milky Way’s Populations of Visible Stars*

Most of the visible stars in our galaxy belong to a **Thin Disk**. The disk’s mass density is exponentially distributed with a characteristic radial scale  $r_D \simeq 3.5$  kpc and a scale height of  $H \simeq 100$  pc for the very young stars and gas, and  $\simeq 325$  pc for older stars. The Thin Disk rotates at a constant  $v_{tDisk} \simeq 220$  km/s and its velocity dispersion is small, of the order of 20 km/s near the Sun and somewhat larger towards the galactic centre.

The faint stars of the Thin Disk may contribute to microlensing. As a typifying example, consider a main-sequence star of mass  $\leq 0.3 M_\odot$  located at a distance of 1 kpc: its apparent luminosity would be smaller than that of the stars being monitored in the LMC. Since the Thin Disk mass function (Scalo 1986) is known, we shall explicitly and separately compute their microlensing effects<sup>3</sup>.

Gilmore and Reid (1983) fitted observations of stellar photometry to a superposition of two exponential disks, and found evidence for the existence of a new galactic component, the **Thick Disk**, to which they attributed a

---

<sup>3</sup> We neglect White Dwarfs, whose contribution to the local column density is less than 20% of that of main-sequence stars (Bahcall 1984).

scale height  $H = 1.5$  kpc and a dispersion velocity  $\sigma_z \simeq 60$  km/s. It is now believed that these measurements were contaminated by stars in the Spheroid (to be discussed anon), and that a proper treatment of the Thick Disk leads to  $H \simeq 1\text{--}1.2$  kpc and  $\sigma_z \simeq 40$  km/s (see for example Freeman 1987 and references therein). The Thick Disk rotates more slowly than the Thin Disk, with  $v_{TDisk} \equiv v_{tDisk} - v_{drift}$ , where  $v_{drift} \simeq 50$  km/s is the “drift” velocity relative to the Thin Disk’s rotation.

The stars in the Thin Disk are of Population I: young and metal-rich. The Thick Disk stars have intermediate metallicities and hence are older than Thin Disk stars. The nature of the Thick Disk is controversial, it may be a tail of the Thin Disk, formed as the older stars were scattered to larger speeds; it may be a star population born in some other way.

The existence of the **Spheroid**, yet another stellar component of the Galaxy, is implied by star counts at high latitudes and by observations of nearby, high-velocity stars. Its density profile is approximately spherical, falling roughly as  $r^{-3.5}$ . The Spheroid is dominantly supported by the large velocity dispersion of its constituents ( $\sigma \simeq 120$  km/s) and has a negligible bulk rotation. It is made of old and metal-poor stars and believed to have been formed in the first  $10^9$  years of the Milky Way’s “protogalactic” life.

### *c) Dark Mass in the Disks and Spheroid*

To estimate the backgrounds to a putative microlensing signal by compact objects in the galactic Halo, we need to know the dark constituency of the observed stellar populations. This is something that, almost by definition, we do not know. There are, however, two handles on this problem. One concerns the extrapolation of the mass functions of observed stars downwards in mass into the region of faint or unlit objects. No such extrapolation is to be trusted; we only discuss this subject for its subliminal worth, letting the dark mass functions we employ in the microlensing predictions vary over a large domain of possibilities.

The second handle on the dark mass of the established stellar distributions concerns the comparison of their visible and “dynamical” masses, and is more secure. The observed galactic rotation curve and velocity dispersions imply upper limits on the local column density  $\Sigma$ , the total mass in a cylinder of unit area extending perpendicularly to the galactic plane to an explored

height of some  $\pm 1.1$  kpc. Subtraction of the column density of observed stars translates into a normalization of the allowed local dark-mass density of a star population with an assumed spacial distribution. The use of this constraint is simplified by the fact that we are not after a precise number, but after a sort of “maxi-estimate” of the non-Halo dark-mass backgrounds to microlensing. We shall normalize the dark mass of the Thin and Thick Disks, independently and in turn, to our maxi-estimate of the dark local column density. In the case of the Spheroid, which contributes little to  $\Sigma$ , we exploit directly the comparison of observations of its luminous and dynamical mass.

The mass function of the main sequence stars in the Thin Disk is known almost down to the hydrogen burning limit  $M_{HB} \simeq 0.085 M_{\odot}$  (Scalo 1986), and follows the “Salpeter law”  $dn/dm \propto m^{-2.3}$  for masses larger than  $\sim 2 M_{\odot}$ . Towards lower masses the mass function flattens, and a smooth continuation into the Brown-Dwarf domain ( $m < M_{HB}$ ) might suggest a relatively small dark component of the Thin Disk<sup>4</sup>. Little is known about the mass function of Thick Disk stars.

Measurements of the Galaxy’s rotation curve imply a local column density in a disk component,  $\Sigma$ , inferior to  $\sim 100 M_{\odot}/\text{pc}^2$  (Binney & Tremaine 1987). Kuijken and Gilmore (1989 a,b), from measurements of dispersion velocities at altitudes  $|z| < z_{max} = 1.1$  kpc, infer a total (disk plus halo) column density  $\Sigma \{|z| < z_{max}\} = (71 \pm 6) M_{\odot}/\text{pc}^2$ . The rotation-curve constraint implies that for the disk alone  $\Sigma_{Disk} \{|z| < z_{max}\} = (48 \pm 9) M_{\odot}/\text{pc}^2$ . Gould (1990) reanalyses the same data to obtain  $\Sigma_{Disk} \{|z| < z_{max}\} = (54 \pm 8) M_{\odot}/\text{pc}^2$ . We choose as a conservative upper bound  $\Sigma_{Disk} \{|z| < z_{max}\} = 75 M_{\odot}/\text{pc}^2$  (Sackett and Gould (1993) make this choice for the total disk column density, while Gould, Miralda-Escudé and Bahcall (1994) overpass the quoted analysis to adopt  $\Sigma_{Disk} = 100 M_{\odot}/\text{pc}^2$ ).

To obtain the maximum allowed dark-matter component, one must subtract from the total column density the various visible contributions. These are approximately  $10 M_{\odot}/\text{pc}^2$  in gas,  $30 M_{\odot}/\text{pc}^2$  in main sequence stars<sup>5</sup>, and  $5 M_{\odot}/\text{pc}^2$  in white dwarf stellar remnants and red giants (Bahcall 1984). For a Thin Disk essentially all the mass is within  $|z| < 1.1$  kpc, while for a Thick

---

<sup>4</sup> A Thin Disk population of infrared-emitting Brown-Dwarfs is significantly bounded by the IRAS survey measurements (Kerins & Carr 1994).

<sup>5</sup> This is also what results from the integration of the Scalo mass function, corrected in order to account for binary stars as in Bahcall (1984).

Disk of scale height  $H \sim 1$  kpc only  $\sim 2/3$  of the column density would be within those heights. Accordingly, we choose for the total dark column densities  $\Sigma_{Thin} = 30M_{\odot}/\text{pc}^2$ ,  $\Sigma_{Thick} = 45M_{\odot}/\text{pc}^2$ .

Let  $R = \sqrt{x^2 + y^2}$  and  $z$  be cylindrical coordinates for the radial and altitude coordinates of the Disks. We parametrize their dark-mass distributions as:

$$\rho(R, z) = \rho_D e^{(R_{\otimes} - R)/r_D} e^{-|z|/H}, \quad (3)$$

with  $R_{\otimes} = 8.5$  kpc,  $r_D \simeq 3.5$  kpc, and  $\rho_D = \Sigma_{dark}/(2H)$  the local dark-mass density. For the Thin and Thick Disk's scale heights we adopt  $H = 325$  pc and  $H = 1.2$  kpc, respectively.

The luminous mass of the Spheroid is  $(1 \text{ to } 3) \times 10^9 M_{\odot}$  (Bahcall, Schmidt and Soneira 1983), while its dynamical mass is modelled to be  $(5 \text{ to } 7) \times 10^{10} M_{\odot}$  (Caldwell and Ostriker 1981, Rohlfs and Kreitschman 1988). This indicates that a large fraction of the Spheroid is in non-luminous Brown-Dwarfs or stellar remnants. The mass function of Spheroid field stars increases steeply<sup>6</sup> towards low masses (Richer and Fahlman, 1992), behaving as  $dn/dm \propto m^{-4.5 \pm 1.2}$  in the interval extending from  $0.14 M_{\odot}$ , the minimum observed masses, to  $0.5 M_{\odot}$ . It suffices to extrapolate these observations down to  $\sim 0.04 M_{\odot}$  (half the hydrogen-burning limit) to get the Spheroid's total dynamical mass. In this sense Brown-Dwarfs are well motivated constituents of the dark mass of the Spheroid.

For the Spheroid's mass distribution we use a simplified expression, in good agreement with the ones used in dynamical fits (Ostriker & Caldwell 1982, Rohlfs & Kreitschman 1988):

$$\rho(r) = \rho_s \left( \frac{R_{\otimes}^{1/2} + b^{1/2}}{r^{1/2} + b^{1/2}} \right)^7, \quad (4)$$

with  $b = 0.17$  kpc and  $\rho_s = 1.5 \times 10^{-3} M_{\odot}/\text{pc}^3$  chosen to give, upon integration, a total dark mass of  $5.7 \times 10^{10} M_{\odot}$  in the Spheroid. The inner 1 kpc of this Spheroid model, which mass is  $\sim 10^{10} M_{\odot}$ , may be identified with the galactic Bulge (Blanco & Tondrup 1989, Blitz & Spergel 1991a)<sup>7</sup>.

---

<sup>6</sup> The luminosity function used by Richer and Fahlman (1992), and hence the results of their analysis, have been criticized by Bahcall *et al.* (1994).

<sup>7</sup> Some observations suggest an additional “nuclear Bulge” (Rich 1990, Kent 1992), pre-

*d) Visible stars and dark-matter in the Large Magellanic Cloud*

May dim or lightless objects located in the LMC itself contribute to microlensing of the LMC stars? (Gould 1993, Wu 1994, Sahu 1994). In discussing this subject, as in the case of our Galaxy, it is useful to recall what is known about visible stars in the LMC.

The luminous component of the LMC is usually described as a flat exponential **Disk** that is seen nearly face-on (determinations of the inclination angle range from  $27^\circ$  to  $45^\circ$ ). The disk's radial scale is  $r_{LMC} \simeq 1.6$  kpc. The question of its scale height is more involved.

The LMC gas and star-clusters have a small velocity dispersion ( $\sigma < 10$  km/s). “Intermediate” (more evolved) populations – planetary nebulae, CH stars and intermediate long-period variables – have  $\sigma \simeq 20$  km/s, characteristic of a Disk population with a scale height  $h \simeq 0.5$  kpc. The older population of long-period variables (OLPV) has a velocity dispersion of  $\sigma \simeq 33$  km/s (Hughes, Wood and Reid 1991), corresponding more closely to a spheroidal distribution than to a disk-like one. Due to a partially-rotational support, this **Spheroid** should be quite flattened, with a minor- to major-axial ratio  $c/a = 0.3$  to  $0.5$ . The spatial distribution resulting from the OLPV counts behaves as  $\sim r^{-1.8}$ .

The LMC's rotation curve is that of a solid body up to a radius of  $\sim 2$  kpc. At larger distances the rotational velocity flattens to an approximately constant 80 km/s (Westerlund 1991 and references therein). The total mass of the LMC inside a radius of 6 kpc, inferred from the rotation curve, is  $M_{LMC} \simeq 6 \times 10^9 M_\odot$ . Larger total masses, as high as  $2 \times 10^{10} M_\odot$ , are obtained if the flat rotation curve is extrapolated up to a distance of 15 kpc, as the velocity of three outlying globular clusters would suggest doing (Storm and Carney 1991, Schommer *et al.* 1992). If this large mass is accounted for by a conventional spherical **Halo**, its density distribution should behave as  $r^{-2}$  and its dispersion would be  $\sigma \simeq 80/\sqrt{2}$  km/s.

We consider the possible additional contribution to the LMC microlensing rates of three different dark stellar populations in the LMC itself:

---

sumably a galactic bar (Blitz and Spergel 1991b, Binney *et al.* 1991). Kiraga & Paczyński (1994) discuss this stellar distribution; in Kent's (1992) model it entails a microlensing rate comparable to that of the inner Spheroid considered by us.

A spherical **Halo** with a scale of  $a = 1$  kpc and a density profile:

$$\rho(r) = \rho_H \frac{a^2}{r^2 + a^2} \theta(r - r_{max}) \quad (5)$$

with  $r_{max} = 10$  kpc and a total dark-mass of  $10^{10} M_\odot$ , chosen as compromises of the various bits of information. The corresponding density is  $\rho_H = 0.09 M_\odot/\text{pc}^3$ .

A **Disk** distribution similar to that of the “intermediate” population objects. We choose its density profile, in cylindrical coordinates, to be:

$$\rho(R, z) = \rho_D e^{-R/r_D} \text{sech}^2\left(\frac{z}{h}\right), \quad (6)$$

where  $r_D = 1.6$  kpc,  $h = 0.43$  kpc and  $\rho_D = 0.29 M_\odot/\text{pc}^3$ , corresponding to an assumed total dark mass of  $4 \times 10^9 M_\odot$  in the disk.

A flattened **Spheroidal** distribution similar to that of the OLPV, normalized to a total dark mass of  $4 \times 10^9 M_\odot$  inside  $r_s = 6$  kpc. Its density function is assumed to be:

$$\rho(R, z) = \rho_s \frac{b^2}{b^2 + \xi^2} \theta(\xi - r_s), \quad \xi \equiv \sqrt{R^2 + \frac{z^2}{\cos^2 \Psi}}, \quad (7)$$

where the ellipticity is  $\cos \Psi \equiv c/a = 0.5$ ,  $b = 1$  kpc, and  $\rho_s = 0.09 M_\odot/\text{pc}^3$  for the presumed total dark mass.

None of the above LMC dark-mass scenarios is defensible to a level of confidence comparable to the analogous scenarios in the Galaxy. We discuss them only to illustrate in some detail how their effects on microlensing are relatively small. When considering a possible addition of invisible LMC objects to those of the dark populations of the Galaxy, a certain degree of consistency is called for. It would be peculiar, for instance, to assume that the halo of the LMC is made of some inscrutable form of “particle” dark matter while that of the Galaxy is baryonic.

### 3 Dark-Mass Mass Functions

Let  $dn(x)/dm$  be the dark-mass function: the number of somber objects with mass between  $m$  and  $m + dm$  at a given point  $x$  in the Galaxy or in

its Halo. Very little is known about the explicit  $m$  and  $x$  dependence of this object, besides the constraints on its integral over all masses, discussed in the previous section. To explore microlensing predictions a measure of definiteness – and of guesswork – are required.

For every dark-mass population we make a **factorization hypothesis**:  $dn(x)/dm$  is the product of a distribution  $dn_0/dm$  depending only on  $m$ , times the pertinent dark-mass density profile:

$$\frac{dn(x)}{dm} = \frac{\rho(x)}{\rho_0} \frac{dn_0}{dm}, \quad (8)$$

where we have used a local density  $\rho_0$  as a normalization. For the very extensive galactic Halo this is a fairly strong conjecture, while for the dark component of the various known stellar distributions, that are multifarious, more localized and better understood, the supposition sounds like an eminently reasonable approximation.

The factorization hypothesis reduces our task to that of speculating on the functional form of  $dn_0/dm$ . We posit two families of ansatze, one very simple, the other quite sensible. The first hypothesis is that of mass functions peaked at a particular mass  $m_0$ :

$$\frac{dn_0}{dm} = \rho_o \frac{\delta(m - m_0)}{m_0}; \quad (9)$$

the second is that of a power-law distribution, of index  $\alpha$ , in the range  $m_1 < m < m_2$ :

$$\frac{dn_0}{dm} = \rho_o \frac{m^{-\alpha}}{D} \theta(m - m_1) \theta(m_2 - m), \quad D \equiv \int_{m_1}^{m_2} m^{1-\alpha} dm, \quad (10)$$

with  $\alpha$  any positive or negative number. We let  $m_i, i = 0, 1, 2$ , lie anywhere in a range  $m_{min}$  to  $m_{max}$ . A plausible value for  $m_{min}$  is given by the Jeans limit, and we follow Low & Lynden-Bell (1976) in choosing  $m_{min} = 7 \times 10^{-3} M_\odot$ , though values as low as  $4 \times 10^{-3} M_\odot$  are possible (Palla, Salpeter & Stahler 1983). For  $m_{max}$  we take a generous hydrogen-burning limit of  $m_{max} = 10^{-1} M_\odot$ .

In the study of microlensing observables, we let the dark-mass functions  $dn_0/dm$  vary over the entire range of possible values of  $m_i$  and  $\alpha$ .

## 4 Microlensing Rates and Time Moments

Let  $L$  be the distance to a source that is microlensed by an object of mass  $M$  crossing close to the line of sight at distance  $x$  from the observer. Follow Einstein in defining a radius that characterizes the gravitational lensing scale:

$$R_E \equiv \sqrt{\frac{GM(L-x)x}{Lc^2}}. \quad (11)$$

Define  $u$  as the distance of the lens to the line of sight in  $R_E$  units:

$$u^2(t) \equiv \left(\frac{l}{R_E}\right)^2 + \left(\frac{v^\perp(t-t_o)}{R_E}\right)^2, \quad (12)$$

with  $t_0$  the time of closest approach,  $l$  the impact parameter, and  $v^\perp$  the modulus of  $\vec{v}^\perp$ , the projection on the plane orthogonal to the line of sight of the relative velocity between the lens and this very line (hereafter, the label “ $\perp$ ” always refers to this projection).

The microlensing amplification of the luminosity of the source is:

$$A[t] = \frac{u^2(t) + 2}{u(t) \sqrt{u^2(t) + 4}}. \quad (13)$$

The maximum amplification,  $A_{max} = A(u_{min})$ , occurs at time  $t = t_0$ , as  $u$  reaches its minimum value  $u_{min} \equiv u(t_0) = l/R_E$ .

The amplification curve  $A[t]$  is universal, its shape is fully determined by its height  $A_{max}$  and its duration  $T \equiv R_E/v^\perp$ . For observations in a given direction, the distribution of events in  $A_{max}$  tests the hypothesis that the distribution of impact parameters ought to be uniform (all the scale lengths characterizing the dark-mass distributions are much bigger than the conceivable Einstein radii). The distribution of event durations  $T$  is pregnant with interesting but well convoluted information, which we aim to extract. The values of  $t_0$  in Eq. (12) are only relevant to the anthropological question of discovery priorities.

Let  $u_{th}$  be the smallest value of  $u_{min}$  for which the amplification is sufficient for an event to be detectable (e.g.  $u_{th} = 1$  corresponds to a detection amplification threshold  $A_{max} > 1.34$ ). Define a microlensing tube of radius

$u_{th} R_E$  around the line of sight. Consider a circle on the tube's surface and let  $\alpha$  be the angle defining a point on this circle, with  $\alpha = 0$  a matter of choice. Let  $\phi$  be the angle between  $\vec{v}^\perp$  and the transverse direction defined by  $\alpha$ . The *microlensing rate*,  $\Gamma$ , is the flux of lenses through the microlensing tube:

$$d\Gamma = u_{th} \cos \phi v^\perp f(\vec{v}) d\vec{v} d\alpha R_E(x) \frac{dn(x)}{dm} dx dm N(L) dL^3, \quad (14)$$

where  $N(L)$  is the number-density of sources and  $f(\vec{v})$  is the distribution of relative velocities between the lenses and the tube. Given the multitude of components of  $\vec{v}$ , the description of  $f(\vec{v})$  is laborious.

We work in a non-rotating, centre-of-mass system of the Galaxy. At the point  $x$  along the line of sight, the microlensing tube “ $\mu lt$ ”, cantilevered from both ends, is moving at a speed:

$$\vec{v}_{\mu lt} = (x/L) \vec{v}_s + (1 - x/L) \vec{v}_\odot, \quad (15)$$

with  $\vec{v}_\odot$  the solar system velocity and  $\vec{v}_s$  the source velocity.

#### *a) Microlensing of LMC and SMC stars by galactic objects*

Consider first the case of observations in the direction of the Magellanic Clouds, for which it is a very good approximation to simplify  $d\Gamma$  in Eq. (14) in two ways. First, the spread in distances to the sources is small enough to forsake the  $N(L) dL^3$  factor. Second, the rotation and dispersion of the source stars are negligible. It is therefore sufficient to keep the overall motion of the Clouds<sup>8</sup> in the source velocity  $\vec{v}_s$  appearing in Eq. (15), and to proceed to the discussion of the velocity distribution of the lensing objects.

In general, the velocity of the lenses  $\vec{v}_{lens}$  consists of a global rotation  $\vec{v}_{lrot}$ , plus a dispersive component  $\vec{v}_{ldis}$  whose distribution we assume to be isotropic and Maxwellian:

$$f(v_{ldis}) = \frac{1}{(2\pi)^{3/2} \sigma_{ldis}^3} \exp \left[ \frac{-v_{ldis}^2}{2 \sigma_{ldis}^2} \right], \quad (16)$$

with  $\sigma_{ldis}$  the dispersion. This describes the motion of sources in a Thin or a Thick Disk, while for the Halo or Spheroid  $\vec{v}_{lrot}$  can be neglected.

---

<sup>8</sup> Griest (1991) shows that this motion corrects the microlensing rates only at the 10% level.

Finally, the relative velocity  $\vec{v}$  between the lens and the microlensing tube, occurring in the microlensing rate of Eq. (14), is:  $\vec{v} = \vec{v}_{lens} - \vec{v}_{\mu lt} = \vec{v}_{lrot} + \vec{v}_{ldis} - \vec{v}_{\mu lt}$ . Solve this expression for  $\vec{v}_{ldis}$ , substitute in Eq. (14), change the  $v^\perp$  variable first to  $T = R_E/v^\perp$ , and then to  $z \equiv R_E/(\sqrt{2}\sigma_{ldis}T)$ , to obtain:

$$\frac{d\Gamma}{dT} = u_{th} \sigma_{ldis}^2 \int_0^\infty dm \int_0^L dx \frac{dn(x)}{dm} z^4 e^{-(z^2+\eta^2)} I_0(2\eta z), \quad (17)$$

where  $\eta(x) \equiv |\vec{v}_{\mu lt}^\perp(x) - \vec{v}_{lrot}^\perp|/(\sqrt{2}\sigma_{ldis})$  and  $I_0$  is the zeroth-order Bessel function.

For the sake of elegance, we consider first the idealized case in which the observational efficiency as a function of event duration,  $\epsilon(T)$ , and the threshold amplification,  $u_{th}(T)$ , have approximately constant values,  $\bar{\epsilon}$  and  $\bar{u}_{th}$ . When discussing observations in the next Section, we illustrate the effects of lifting the first (and more unrealistic) of these hypothesis. The second we also revoke in the discussion of actual data, in Section 6d.

Upon use of the factorization hypothesis, Eq. (8), the total rate  $\Gamma$  deconvolutes into the product of two terms, one depending only on the mass function, the other on the dark density profile:

$$\Gamma = \frac{\bar{\epsilon} \bar{u}_{th} \sigma_{ldis}}{\rho_0} \sqrt{\frac{8\pi G}{c^2 L}} \int_0^\infty dm \sqrt{m} \frac{dn_0}{dm} \int_0^L dx \rho(x) \sqrt{x(L-x)} \frac{e^{-\eta^2/2}}{\eta} M_{-1,0}(\eta^2), \quad (18)$$

where  $M_{\mu,\nu}$  are the Whittaker functions. The average duration,  $\langle T \rangle$ , and other duration moments,  $\langle T^n \rangle$ , of the  $d\Gamma/dT$  distribution also factorize:

$$\langle T^n \rangle \equiv \frac{1}{\Gamma} \int_0^\infty dT T^n \frac{d\Gamma}{dT} = \left( \frac{2G}{c^2 L} \right)^{\frac{n}{2}} \frac{1}{\sigma_{ldis}^n} \frac{\mathcal{M}_n}{\mathcal{M}_0} \frac{\mathcal{X}_n}{\mathcal{X}_0}, \quad (19)$$

where:

$$\mathcal{M}_n \equiv \int_0^\infty dm m^{\frac{1+n}{2}} \frac{dn_0}{dm}, \quad (20)$$

$$\mathcal{X}_n \equiv \Gamma \left( \frac{3-n}{2} \right) \int_0^L dx \rho(x) [x(L-x)]^{\frac{1+n}{2}} \frac{e^{-\eta^2/2}}{\eta} M_{\frac{n}{2}-1,0}(\eta^2). \quad (21)$$

Equations (18–21) imply that, for a known density and velocity distribution of the lensing objects, it is possible to extract their mass function—in the

sense of its moments— from the observed distribution of event durations (De Rújula, Jetzer & Massó 1991).

We shall concentrate on the information contained in the total rate  $\Gamma$  and its  $n = 1, 2$  time-moments, for which we beg to recall that  $M_{-\frac{1}{2},0}(y) = \sqrt{y} e^{y/2}$  and  $M_{0,0}(y) = \sqrt{y} I_0(y/2)$  with  $I_0$ , once again, a Bessel function. It will prove useful to combine the  $n = 1$  and  $n = 2$  time-moments into a time dispersion:

$$\frac{\Delta T}{T} \equiv \frac{\sqrt{\langle T^2 \rangle - \langle T \rangle^2}}{\langle T \rangle}, \quad (22)$$

characterizing the spread of event durations around their mean.

*b) Microlensing of LMC stars by dark objects in the LMC*

In the appraisal of LMC “backgrounds” to a putative galactic-Halo signal, several simplifications are good approximations. The microlensing rates are only slightly underestimated by placing the sources in the plane of a disk and neglecting its inclination, so as to view it from “above”. The velocity dispersion of the source stars can be neglected relative to that of the lenses. Finally, the rotation of the sources can also be ignored. It has no effect in the case of a dark disk component, for which sources and lenses rotate abreast. Moreover, MACHO observes the inner 1.5 kpc of the LMC, while the EROS plates portray the inner 2.5 kpc. There, rotation is small; its inclusion would only slightly increase the rate and reduce the durations of the predicted LMC dark Halo and Spheroid backgrounds.

The microlensing rate and time moments depend on the angle between the monitored stars and the centre of the LMC disk, an effect that is not negligible for lenses in the LMC itself. Accordingly, we weigh the predictions for each observable  $\mathcal{O}$  with the radial distribution of sources in the LMC disk,  $n(R)$ , and average over the observed fields:

$$\langle \mathcal{O} \rangle = \frac{\int_0^{R_{max}} n(R) \mathcal{O}(R) dR^2}{\int_0^{R_{max}} n(R) dR^2}. \quad (23)$$

Here, we use  $n(R) = e^{-R/h}$ ,  $h = 1.6$  kpc, and  $R_{max} = h$ , roughly the field of view of the MACHO collaboration<sup>9</sup>.

---

<sup>9</sup> Averaging as in Eq. (23) mitigates the uncertainty arising from the LMC Halo or Spheroid core radii.

*c) Bulge observations*

The microlensing predictions for observations in the general direction of the galactic centre (Paczynski 1991, Griest *et al.* 1991) are sensitive to two effects that are negligible for the Magellanic Clouds: the dispersion of source velocities and their spread of distances along the line of sight. We include these effects in our predictions, even though they are presumably smaller corrections than those to be made hand in hand with the foreseeable improvements of our knowledge of the star distributions in, around and towards the Bulge.

Bulge stars have a Maxwellian distribution of velocities  $v_{Bdisp}$  with dispersion  $\sigma_B \simeq 100$  km/s. They probably rotate jointly at a speed  $v_{Brot} \simeq 100$  km/s, but their density along the line of sight peaks close to the galactic centre, where  $v_{Brot}^\perp \sim 0$ , so that the effects of rotation on microlensing observables can be neglected. The velocity dispersion is taken into account by computing the microlensing rate and time-moments from the convolution of the  $v_{Bdisp}$  distribution and a function  $d\Gamma_B/dT$  of the same form as that of Eq. (17):

$$\frac{d\Gamma_B}{dT} = \frac{1}{2\pi\sigma_B^2} \int_0^{2\pi} d\theta \int_0^\infty dv_B v_B \frac{\widetilde{d\Gamma}}{dT} \exp\left(-\frac{v_B^2}{2\sigma_B^2}\right), \quad (24)$$

where  $v_B = |\vec{v}_{Bdisp}^\perp|$  and  $\theta$  is the angle between  $\vec{v}_{Bdisp}^\perp$  and  $\vec{V} = (1 - x/L) \vec{v}_\odot^\perp - \vec{v}_{lrot}^\perp$ . The tilde over  $d\Gamma/dT$  is to remind one to use Eq. (17) with  $\eta(x) = |\vec{V} + (x/L) \vec{v}_{Bdisp}^\perp|/(\sqrt{2}\sigma_{ldis})$ .

The stars monitored in the Bulge are sufficiently disseminated along the line of sight to study lifting the approximation wherein they all reside at  $L = R_\odot$ . To do this, make yet another convolution of the time distribution of Eq. (24):

$$\frac{d\bar{\Gamma}_B}{dT} = \frac{\int (d\Gamma_B/dT) N(L) L^{-2\beta} dL^3}{\int N(L) L^{-2\beta} dL^3}, \quad (25)$$

with  $N(L)$  the source number density along the line of sight and  $L^{-2\beta}$  a correction describing the observability of stars of given luminosity as a function of distance. We choose  $\beta = 1$ , the optimistic endpoint of the range considered by Kiraga and Paczynski (1994) and an  $N(L)$  distribution for the Bulge with the spheroidal shape of Eq. (4).

The average over source locations introduces significant corrections (a  $\sim 25\%$  rate increase of and a  $\sim 20\%$  elongation of event durations) only for lenses in the Spheroid. For this distribution the most probable lens location is close to the galactic centre, enhancing the contribution and Einstein radii of sources at  $L > R_{\odot}$ .

## 5 Results of Gedanken Observations

The multiple microlensing rates as functions of event duration discussed in Section 4 contain the information needed to interpret observations in a hypothetical scenario wherein data are plentiful, experimental efficiencies and visibility thresholds are uniform and well understood, and the modelling of the Galaxy is sufficiently accurate. Before we backtrack a bit from this fleckless idealization, it is useful to plot and compare the different predictions for  $d\Gamma/dT$ . To bracket a large range of possibilities, we choose the exemplars of lensing bodies with fixed masses,  $m_0 = 0.007M_{\odot}$  and  $m_0 = 0.1M_{\odot}$ , the extreme values we have adopted.

In Fig. 2, which refers to LMC observations, we portray the predicted  $d\Gamma/dT$  for lenses in the galactic Halo, Spheroid, and Thin or Thick Disks, as well as for the possible dark populations in the LMC Halo, Disk and Spheroid. Figs. 2a and 2b correspond to the two chosen extreme values of the lensing mass. The time durations of the disk predictions are longer and more peaked than the rest, a consequence of global rotation. The expectation for faint disk stars is also shown in the figures; in its estimate we used the measured mass function (Scalo, 1986), in a mass range extending from the H-burning threshold to  $0.5 M_{\odot}$ .

In the ideal case we are discussing, it is easy to generalize the results of Fig. 2. To predict  $d\Gamma/dT$  for mass functions peaked at some other mass, notice that the height and position of its peaks respectively scale as  $1/m_0$  and  $\sqrt{m_0}$ , while the shape of the curves, in a log-log plot, is  $m_0$ -independent. Wider mass functions widen the predicted time distributions in ways to be characterized in detail in the next Section.

Figure 3 is the Baade-window counterpart of Fig. 2. For the models we consider, the predictions for the other fields observed by OGLE in the

Table 1: Event rate  $\Gamma$  (for  $10^7$  star-years of observation and  $u_{th} = 1$ ) and mean event duration  $\langle T \rangle$  (in days) for 100% efficient microlensing searches in the LMC and Baade’s window. The average distances to the lenses (in kpc) is  $\langle x \rangle$ . The symbol  $m_{.05}$  stands for  $m/0.05M_{\odot}$ .

Source	Observable	Halo	Spheroid	Thick Disk	Thin Disk
LMC	$\Gamma$	$92/\sqrt{m_{.05}}$	$6.8/\sqrt{m_{.05}}$	$5.5/\sqrt{m_{.05}}$	$1.1/\sqrt{m_{.05}}$
	$\langle T \rangle$	$15\sqrt{m_{.05}}$	$16\sqrt{m_{.05}}$	$20\sqrt{m_{.05}}$	$23\sqrt{m_{.05}}$
	$\langle x \rangle$	15	9.2	3.6	1.1
Bulge	$\Gamma$	$11/\sqrt{m_{.05}}$	$31/\sqrt{m_{.05}}$	$8.5/\sqrt{m_{.05}}$	$10/\sqrt{m_{.05}}$
	$\langle T \rangle$	$5.8\sqrt{m_{.05}}$	$5.6\sqrt{m_{.05}}$	$11\sqrt{m_{.05}}$	$11\sqrt{m_{.05}}$
	$\langle x \rangle$	5.6	7.7	6.2	5.7

direction of the Bulge are very similar to the ones of Fig. 3. Notice that, contrary to observation, most of the expected events have time durations shorter than  $\sim 15$  days, irrespective of the dark population responsible for them.

In Table 1 we list the values of  $\Gamma$  and  $\langle T \rangle$  for mass functions peaked at a single mass, for observations in the LMC and in Baade’s Window. We also give the quantities

$$\langle x \rangle \equiv \frac{1}{\Gamma} \int_0^L dx \frac{d\Gamma}{dx} x, \quad (26)$$

defining, for each dark-mass population, the average distance from the solar system at which microlensing takes place.

## 6 Towards the Analysis of Realistic Data

Microlensing observations are unlikely to accumulate in the near future at a rate faster than a few dozen events per year. May such a relatively modest body of data answer the burning question of the nature of the dark mass of

our galactic Halo? We cannot answer this question a priori, but we examine simple strategies to eke out the information buried in the data. The nine events already gathered by OGLE in the Bulge direction are sufficient to start testing these strategies.

The first observables of interest are the rate of events  $\Gamma$  and their mean duration  $\langle T \rangle$ . Their product, or the optical depth  $\tau = (\pi/2) u_{th} \Gamma \langle T \rangle$ , has the advantage of being, unlike its factors, independent of the mass function of the lenses (since it is difficult to assess meaningful error ranges to the various uncertainties, it is important to individuate the inputs to which the distinct observables are *not* sensitive).

As the data accumulate, more detail of the  $T$ -distribution will become statistically significant, starting with the spread in event durations  $\Delta T/T$ , defined in Eq. (22). For a fixed dark-mass distribution, the time moments, unlike  $\Gamma$ , are insensitive to the overall dark-mass normalization, their uncertainty stems from that of the assumed rotational and dispersive velocities. For LMC and SMC observations, the predictions for  $\Delta T/T$  are quite insensitive to dispersion, and are therefore particularly solid for lenses in a spherical Halo or Spheroid, that have no collective rotation.

#### *a) LMC observations*

We present predictions for the Halo signal and the various backgrounds in the form of two plots,  $\Gamma$  versus  $\langle T \rangle$ , and  $\Delta T/T$  versus  $\langle T \rangle$ . The first of these, for the LMC, is Fig. 4. In Fig. 4a the observational efficiency is assumed to be ideal,  $\epsilon(T) = 1$ , and the amplification threshold is chosen to be a uniform  $u_{th} = 1$ . Since the optical depth ( $\tau \propto \Gamma \langle T \rangle$ ) is independent of the mass function, the predictions for the various components (in a log-log plot) are straight lines with slope  $-1$ . The finite range in  $\langle T \rangle$  derives from the assumed bracketed range of lensing masses<sup>10</sup>. Faint disk stars would give the largest values of  $\langle T \rangle$ , but their rate contribution to LMC microlensing is negligible.

In interpreting Fig. 4a and others to come, it is important to bethink that the uncertainties in the various  $\Gamma$ 's are proportional to those in the assumed

---

<sup>10</sup> The integral of a power-law dark-mass function is dominated by its endpoints,  $m_1$  or  $m_2$ , for  $\alpha > 2$  or  $\alpha < 2$ . The corresponding “critical” exponent for the rate  $\Gamma$  is a sesquialteral  $\alpha = 3/2$ .

dark mass densities, and to recall that for the Halo signal we have taken a central-value density, while for the various backgrounds we have made upper-limit estimates.

In Fig. 4b we illustrate the effects of an  $\epsilon(T) < 1$ , with use of the efficiency attained by the EROS team during the first three years of Schmidt plate observations (Bareyre, private communication). The tilt in the curves stems from that of  $\epsilon(T)$ , which rises with  $T$ . The figure shows how the microlensing rate for a Brown-Dwarf-dominated Halo towers over all backgrounds. EROS and MACHO have each accumulated some  $10^7$  star-yrs of observation, and observed two and three microlensing events, respectively. If their efficiencies are comparable and their detection thresholds correspond to  $u_{th} \sim 1$ , the Halo model would appear to overestimate the event rate by half an order of magnitude, within the currently meager statistics. The actual results could perhaps be explained by a dominantly dark Spheroid (Giudice, Mollerach & Roulet 1994) or Thick Disk (Gould, Miralda-Escudé & Bahcall 1994).

Also shown in Fig. 4 are the predictions for micro-lensing by dark objects in the LMC itself. The contribution of a Halo component would be as much as  $\sim 20\%$  of that of the Milky Way Halo. May the LMC Halo be made of dark massive objects while that of our Milky Way is dominated by something else? If not, the two Brown-Dwarf Halo curves must be added accordingly. In the absence Brown-Dwarf halos, the contribution of an LMC dark Spheroid may not be negligible.

In Fig. 5 we show the results for  $\Delta T/T$  versus  $\langle T \rangle$  for the various galactic dark-mass distributions. Fig. 5a is for a time-independent efficiency and Fig. 5b for the EROS efficiency cited before. For each dark-mass component, the indetermination of the mass function  $dn_0/dm$  results in predictions spread over an area of the  $(\Delta T/T, \langle T \rangle)$  plane: the “Napoleon hats” of the figure. For the single-mass distributions of Eq. (9),  $\Delta T/T$  is independent of  $m_0$ , the lower boundaries of the hats trace the values of  $\langle T \rangle$  as  $m_0$  runs from  $m_{min}$  to  $m_{max}$ . The power-law mass functions of Eq. (10) lead to larger values of  $\Delta T/T$ . The upper hat boundaries are traced for  $m_1 = m_{min}$ ,  $m_2 = m_{max}$ , as  $\alpha$  runs from  $+\infty$  to  $-\infty$ , with the top of the hat at  $\alpha = 2$ . Shorter mass intervals correspond to smaller hats, with the ensemble of mass functions we consider filling the overall allowed domain<sup>11</sup>.

---

<sup>11</sup> The hypothetical LMC backgrounds are not included in Fig. 5. Unlike for the rates

We learn from Fig. 5 that, even with relatively modest statistics and a realistic efficiency, a measurement of the duration spread of the events can help distinguish a Halo signal from the Disk backgrounds, whose non-negligible rotation leads to smaller values of the predicted  $\Delta T/T$ . A galactic Halo signal and the Spheroid background would have to be disentangled on the basis of their different predicted rates, as in Fig. 4.

*b) Comparison of SMC and LMC observations*

The MACHO collaboration has started to look also for microlensing of stars in the SMC. The comparison of the microlensing event rates towards the SMC and the LMC will provide a useful tool to discriminate among the different models of galactic Brown-Dwarf populations. We obtain  $R_{MC} \equiv \Gamma_{SMC}/\Gamma_{LMC} = 1.4, 1.7, 0.9$  and  $0.6$  for the Halo, Spheroid, Thick Disk and Thin Disk respectively<sup>12</sup>. This test is particularly good to distinguish between the Spheroid and Disks models. The SMC is at a smaller angle with respect to the galactic centre than the LMC, making  $R_{MC}$  large for the Halo and Spheroid. The Disk rates are very sensitive to latitude, which is slightly larger for the SMC than for the LMC, explaining the lower values predicted for  $R_{MC}$ .

The expectations for  $d\Gamma/(\Gamma dT)$  are similar for the LMC and the SMC; the ratio  $R_{MC}$  is quite insensitive to the assumed mass functions, and almost independent of the observational efficiencies, provided they are similar for the two Clouds. The value of  $R_{MC}$  is also close to the ratio of optical depths, the quantity discussed by Sackett and Gould (1993) and Gould, Miralda-Escudé & Bahcall (1994). Our Thick Disk result  $R \sim 0.9$  differs from that of Gould, Miralda-Escudé & Bahcall (1994), who did not include a radial dependence of the Disk column density. This is relevant for the Thick Disk, for which microlensing occurs at  $\langle x \rangle = 3.6$  kpc, comparable to the Disk's scale length.

To obtain  $R_{MC}$  we neglected possible contributions from dark lensing objects around the Magellanic Clouds themselves. If such contributions were

---

of Fig. 4, they are not simply additive and a multitude of combinations is possible, all of which result in “hats” that, relative to the ones of Fig. 5, are somewhat stretched towards larger values of  $\langle T \rangle$  and  $\Delta T/T$ .

<sup>12</sup> Sackett and Gould (1993) discuss the usefulness of  $R$  to distinguish halos of different ellipticity and Gould, Miralda-Escudé & Bahcall (1994) to distinguish between the Disk and Halo models.

sizable, estimates of  $R_{MC}$  would actually require a detailed knowledge of the lens distribution in those galaxies, not a readily available piece of information.

*c) Bulge observations*

The predictions for microlensing rates as functions of average times, for observations in the Baade window, are given in Fig. 6. Fig. 6a is for a perfect efficiency, while in Fig. 6b we have used  $\epsilon(T)$  as quoted by the OGLE team (Udalski *et al.* 1994). Dim objects in the Spheroid and Disk populations result in larger event rates than those predicted for the galactic Halo, the transpose of the situation for the LMC depicted in Fig. 4.

In Fig. 7 we show the  $\Delta T/T$  versus  $\langle T \rangle$  plane for the Bulge. Unlike for the LMC case of Fig. 5, it seems much more difficult to discriminate among the different galactic components with measurements of  $\langle T \rangle$  and  $\Delta T/T$ . Also, the effect of the experimental OGLE efficiency strongly modifies the picture, as shown in Fig. 7b. This is caused by the rapidly falling efficiency at small time durations, where the theoretical time distributions are peaked.

The known faint Disk stars complicate the analysis of microlensing in the Bulge direction. If the other dark populations have mass functions not peaked close to  $0.1 M_{\odot}$ , two distinct peaks may arise in the distribution of event durations, otherwise the contribution of faint Disk stars must be handled theoretically.

*d) An inspection of the OGLE data*

In  $1.7 \times 10^6$  star-yrs of observation, the OGLE group has seen 9 events, one of which may be a long-period variable star. Figure (6) shows that the remaining 8 events are in excess of the individual predictions of any of the galactic components, but may be compatible with the largest expectation of  $\sim 5$  events, obtained by adding the rates for the Spheroid, either of the dark Disk models, and the faint stars. The observed  $\langle T \rangle \simeq 20$  days is in the upper end of the expectations, that do not exceed that value for any of the dark-mass models. How significant are these uncomfortable indications? Poissonian statistics suffice to compare the numbers of expected and observed events, but a probabilistic test of a time distribution necessitates a hypothesis on its shape, plus some extra labour.

One of the OGLE events is best interpreted as due to microlensing by a

binary object; it is difficult to include it in an analysis of time durations. The event compatible with a variable star is suspicious and we also discard it, to be left with 7 events. Seven is too small a number for a conventional  $\chi^2$  test of a binned distribution to be safe, we must resort to a Kolmogorov–Smirnov test of the cumulative probability of the observed distribution to agree with the expectation<sup>13</sup>. Since the observed durations are large, the expectations least likely to “fail” are those corresponding to mass functions peaked at a single large mass, justifying the use of a single mass-ansatz. The background of faint stars also corresponds to large durations and we add it to each of the individual dark-mass models.

The results of the above exercise are shown in Fig. 8, where the Kolmogorov–Smirnov probability as a function of lensing mass is shown for each dark population model. The Spheroid and, to a lesser extent, the Halo model fare badly for masses below the hydrogen-burning limit. The Disk models survive this test with flying colours, but fail the rate test of Fig. 6b: in either of them one would expect less than two events for the currently accumulated statistics, the probability of observing 8 or 9 events is totally negligible. Thus the unavoidable need to complicate former models of the inner galaxy.

To face these problems, the MACHO observers (Alcock *et al.* 1994) suggest a very centrally-singular Halo, a maximal Disk and the possible contribution of source stars lying behind the Bulge, with the greater distance to the lensing object increasing the lensing probability and time scale. Members of the OGLE collaboration (Paczynski *et al.* 1994) advocate the effects of the *galactic Bar*, a cigar-like ensemble of stars whose elongated axis would point towards us from the neighbourhood of the galactic centre, at an angle of only  $\sim 15^\circ$  relative to the line of sight (Binney *et al.* 1991). Lensing by dim stars in the Bar would contribute to the large observed event rate; their small apparent transverse velocities would result in relatively long-duration events.

---

<sup>13</sup> In the cumulative probability we use steps at each measured event duration  $T^i$  proportional to the inverse of its individual threshold  $u_{th}^i$ , reported in Udalski *et al.* (1994).

## 7 Conclusions

Microlensing observations are the best current tool to search for compact lumps of baryonic dark-matter in the Galaxy. The observational campaigns were designed to ascertain the extent to which the galactic Halo consists of massive astrophysical objects or, by exclusion, of a more elusive substance. Infrared searches, that we have not discussed, are another tool to locate nearby individual Brown Dwarfs, or their collective glow in another galaxy.

It is becoming increasingly clear that the microlensing observations are sensitive to “backgrounds” of dark objects residing in galactic components other than the Halo, such as the Spheroid and the Thick or Thin Disks. We have presented a detailed description of the microlensing Halo signal and the various backgrounds, an analysis designed to accomodate the foreseeable scarcity of data. Our aim is to pin down the likely location of the lensing objects, as well as to extract the first indications of what their mass function may be.

The observations of the Bulge are intriguing. We have analysed the statistical significance of the discrepancy between the OGLE observations and the expectations for simple dark-mass models and known faint stars, or combinations thereof. In agreement with previous authors (Alcock *et al.*, 1994; Paczyński *et al.* 1994), we conclude that the earlier understanding of the inner galactic realm must be revised. In this connection, microlensing observations with a good sensitivity for short-duration events (10 days or less), for which the expected rates are large, would be very useful. So would the comparison of observations in “windows” located at different latitudes and relative angles to the galactic centre.

Needless to emphasize, even a Brown-Dwarf-dominated galactic Halo would contribute very little to microlensing of Bulge stars, so that observations in that direction are not decisive to the question of the Halo constituency, though they constitute a handle on various microlensing “backgrounds”.

We have argued that for the microlensing of LMC stars, the comparison of data and expectations for the rate, mean event duration and time dispersion should suffice to disentangle the galactic component to which the Brown-Dwarfs belong. A comparison of LMC and SMC rates may also come in

handy.

To summarize, microlensing observations of the galactic Bulge are already significantly contributing to our astrophysical lore; very soon observations of the Magellanic Clouds ought to add to our knowledge of cosmology. The question of the nature of the Halo of our galaxy is still wide open, but the prospects for continuing progress appear to be excellent.

## 8 References

- Alcock C. *et al.*, 1993. *Nature* **365**, 621.
- Alcock C. *et al.*, 1994. Preprint.
- Aubourg E. *et al.*, 1993. *Nature* **365**, 623.
- Bahcall J. N., Schmidt M. & Soneira R. M., 1983. *Astrophys. J.* **265**, 730.
- Bahcall J. N., 1984. *Astrophys. J.* **276**, 169.
- Bahcall J. N. *et al.*, 1994. Preprint.
- Binney, J. & Tremaine, S., 1987. *Galactic Dynamics*, Princeton University Press, Princeton.
- Binney J. *et al.*, 1991. *Mon. Not. R. astr. Soc.* **252**, 210.
- Blanco V. M. & Tendrup D. M., 1989. *Astronom. J.* **98**, 843.
- Blitz L. & Spergel D. N., 1991a. *Astrophys. J.* **370**, 205.
- Blitz L. & Spergel D. N., 1991b. *Astrophys. J.* **379**, 631.
- Caldwell J. A. R. & Ostriker J. P., 1981. *Astrophys. J.* **251**, 61.
- Carswell R. F. *et al.*, 1994. *Mon. Not. R. astr. Soc.*, in press.
- Chandrasekhar, S., 1942. *Principles of Stellar Dynamics*, The University of Chicago Press, Chicago.
- De Rújula A., Jetzer P., & Massó E., 1991. *Mon. Not. R. astr. Soc.* **250**, 348.
- De Rújula A., Jetzer P., & Massó E., 1992. *Astron. Astrophys.* **254**, 99.
- Einstein A., 1936. *Science* **84**, 506.

- Fich M. & Tremaine S., 1991. *Ann. Rev. Astron. Astrophys.* **29**, 409.
- Freeman K. C., 1987. *Ann. Rev. Astron. Astrophys.* **25**, 607.
- Frieman, J. & Scoccimarro, R., 1994. Preprint.
- Gilmore G. & Reid N., 1983. *Mon. Not. R. astr. Soc.* **202**, 1025.
- Giudice G.F., Mollerach S. & Roulet E., 1994. *Phys. Rev. D* in press.
- Gould A., 1990. *Mon. Not. R. astr. Soc.* **244**, 25.
- Gould, A., 1993. *Astrophys. J.* **404**, 451.
- Gould A., Miralda-Escudé J. & Bahcall J. N., 1994. *Astrophys. J.* **423**, L105.
- Graboske H. C. & Grossman A. S., 1971. *Astrophys. J.* **170**, 165.
- Griest K., 1991. *Astrophys. J.* **366** 412.
- Griest K. *et al.*, 1991. *Astrophys. J.* **372**, L79.
- Hughes S. M. G., Wood P. R. & Reid N., 1991. *IAU Symposium "The Magellanic Clouds"*, 15, eds. R. Haynes and D. Milne.
- Kent S. M., 1992. *Astrophys. J.* **387**, 181.
- Kerins E. J. & Carr B. J., 1994. *Mon. Not. R. astr. Soc.* **266**, 775.
- Kiraga M. & Paczyński B., 1994. *Astrophys. J. Letters*, in press.
- Kuijken K. & Gilmore G., 1989a. *Mon. Not. R. astr. Soc.* **239**, 571.
- Kuijken K. & Gilmore G., 1989b. *Mon. Not. R. astr. Soc.* **239**, 605.
- Low C. & Lynden-Bell D., 1976. *Mon. Not. R. astr. Soc.* **170**, 367.
- Ostriker J. P. & Caldwell J. A. R., 1982. In *Dynamics and Structure of the Milky Way*, ed. W. L. H. Shuter, Reidel, Dordrecht.
- Paczynski B., 1986. *Astrophys. J.* **304**, 1.
- Paczynski B., 1991. *Astrophys. J.* **371**, L63.
- Paczynski B. *et al.*, 1994. Preprint.
- Palla F., Salpeter E.E. & Stahler S.W., 1983. *Astrophys. J.* **271**, 632.
- Rich R. M., 1990. *Astrophys. J.* **362**, 604.
- Richer H. B. & Fahlman G. G., 1992. *Nature* **358**, 383.

- Rohlf K. & Kreitschman J., 1988. *Astron. Astrophys.* **201**, 51.
- Sackett P. & Gould A., 1993. *Astrophys. J.* **419**, 648.
- Sackett P. *et al.*, 1994. *Nature* **370**, 441.
- Sahu, K., 1994. Preprint.
- Scalo J. M., 1986. *Fund. of Cosmic Phys.* **11**, 1.
- Schommer R. A. *et al.*, 1992. *Astron. J.* 103, 447.
- Songaila A. *et al.*, 1994. *Nature* **368**, 599.
- Storm J. & Carney B. W., 1991. *IAU Symposium "The Magellanic Clouds"*, 15, eds. R. Haynes and D. Milne.
- Udalski, A. *et al.*, 1994. *Acta Astronomica* **44**, 165.
- Walker T. P. *et al.*, 1991. *Astrophys. J.* **376**, 51.
- Westerlund B. E., 1991. *IAU Symposium "The Magellanic Clouds"*, 15, eds. R. Haynes and D. Milne.
- Wu X.-P., 1994. Preprint.

## 9 Figure Captions

**Figure 1:** On a plane orthogonal to the Galaxy’s equatorial plane, this figure shows the mass density contour lines of  $10^{-2}M_{\odot}/\text{pc}^3$  and  $10^{-3}M_{\odot}/\text{pc}^3$  for the Halo (solid line), the Spheroid (dashed line), the Thick Disk (solid line), and the Thin Disk (dotted line). The location of the Sun is indicated by an asterisk. The Magellanic Clouds lie above the plane, as indicated.

**Figure 2:** The microlensing event distributions in time durations for observations towards the LMC predicted by the various Milky Way and LMC components. All dark objects are assumed to have the same mass,  $M = 0.007M_{\odot}$  in Fig. 2a and  $M = 0.1M_{\odot}$  in Fig. 2b.

**Figure 3:** The analog of Fig. 2 for observations towards the galactic Bulge.

**Figure 4:** The microlensing event rate,  $\Gamma$ , versus the average event duration,  $\langle T \rangle$ , for observations towards the LMC predicted by the various Milky Way and LMC components, with the mass functions varied as in the text and

$u_{th} = 1$ . The asterisk shows the prediction of known faint-disk stars. The efficiency  $\epsilon(T)$  is unity in Fig. 4a and equal to the EROS efficiency for Schmidt plate observations (Bareyre, private communication) in Fig. 4b.

**Figure 5:** The analog of Fig. 4 for the allowed domains in the  $(\langle T \rangle, \Delta T/T)$  plane of average time duration versus time dispersion.

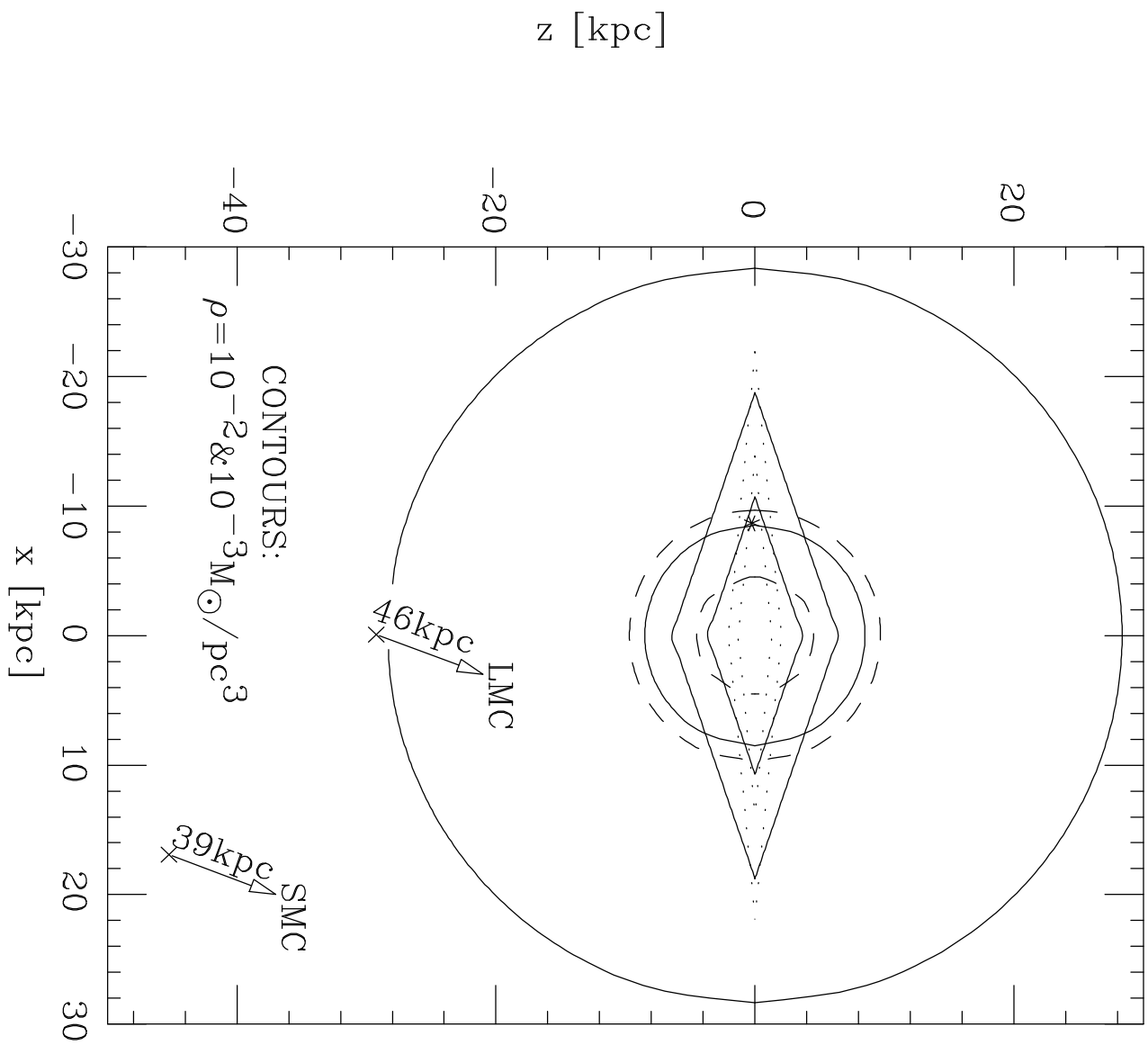
**Figure 6:** The microlensing rate,  $\Gamma$ , versus the average event duration,  $\langle T \rangle$ , for observations towards the galactic Bulge predicted by the different Milky Way components, with the mass functions varied as in the text and  $u_{th} = 1$ . The asterisk shows the prediction of known faint disk stars. The experimental efficiency  $\epsilon(T)$  is unity in Fig. 6a and equal to the OGLE efficiency (Udalski *et al.* 1994) in Fig. 6b.

**Figure 7:** The analog of Fig. 6 for the allowed domains in the  $(\langle T \rangle, \Delta T/T)$  plane of average time duration versus time dispersion.

**Figure 8:** Kolmogorov-Smirnov probability that the OGLE observed distribution of event durations be consistent with the predictions of the different Milky Way dark components, as function of the assumed single lens mass. The faint star contribution has been added to each distinct model.

This figure "fig1-1.png" is available in "png" format from:

<http://arXiv.org/ps/astro-ph/9408099v1>



This figure "fig2-1.png" is available in "png" format from:

<http://arXiv.org/ps/astro-ph/9408099v1>

This figure "fig1-2.png" is available in "png" format from:

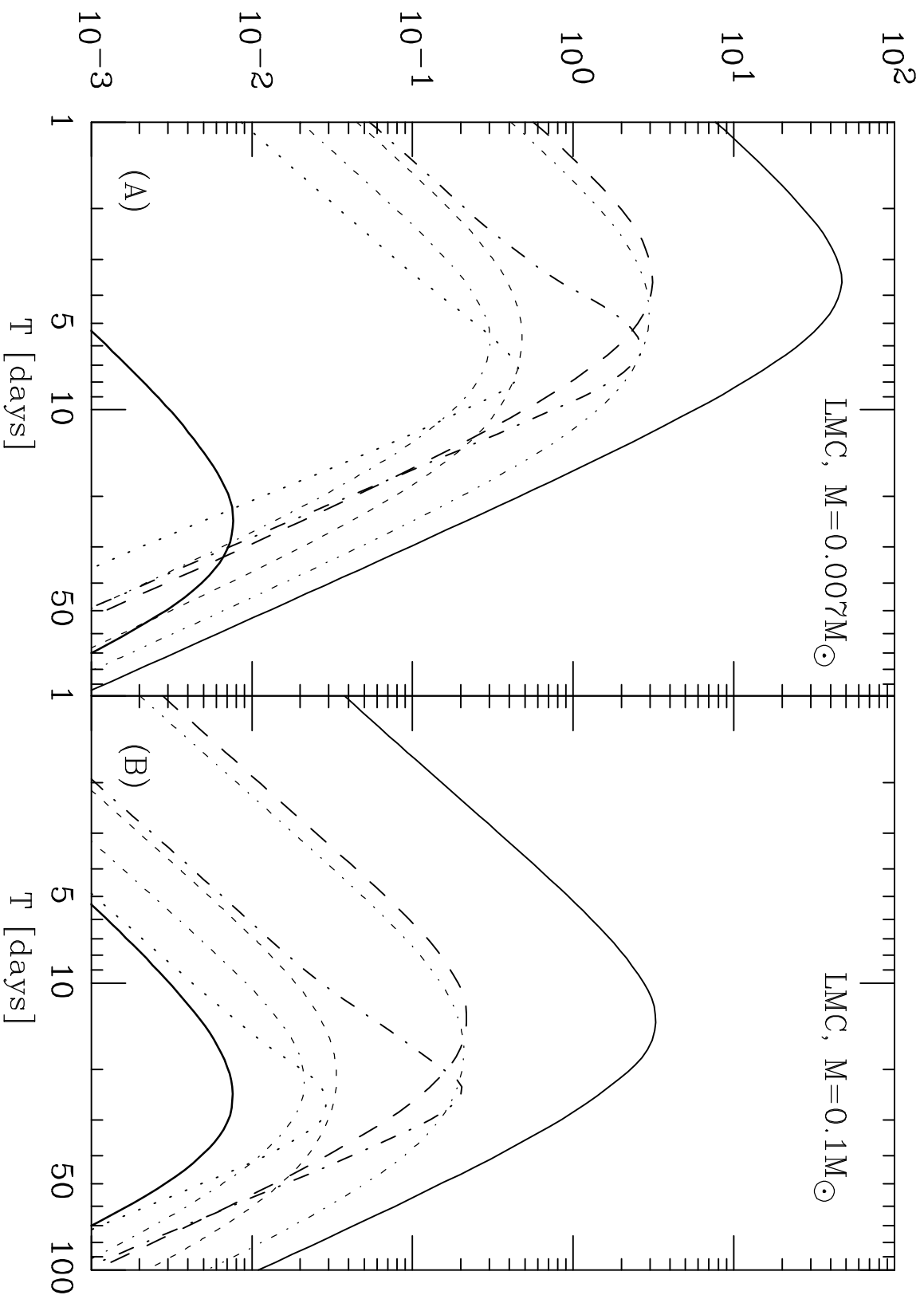
<http://arXiv.org/ps/astro-ph/9408099v1>

This figure "fig2-2.png" is available in "png" format from:

<http://arXiv.org/ps/astro-ph/9408099v1>



$d\Gamma/dT$  [events/( $10^7$  stars yr day)]



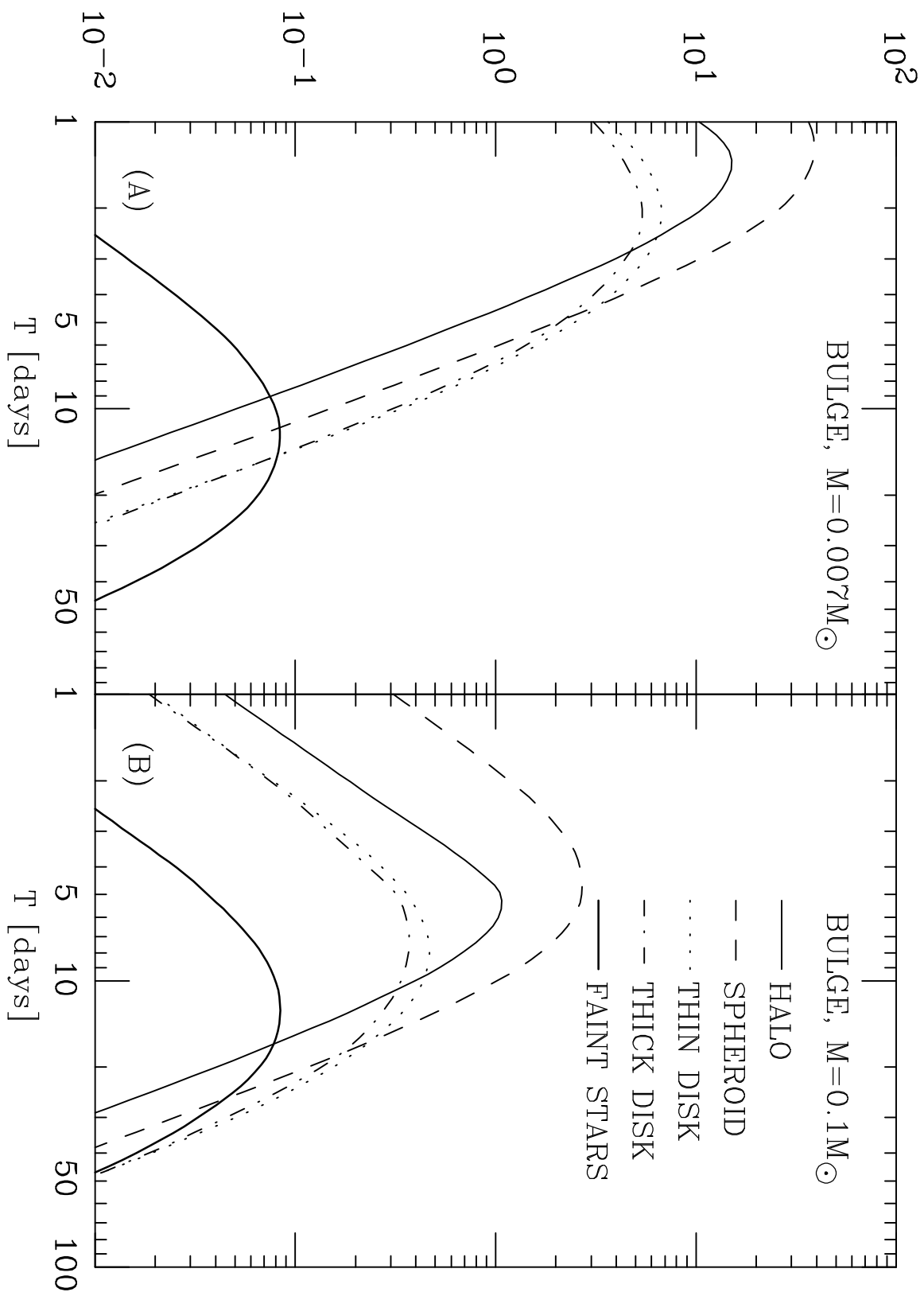
This figure "fig1-3.png" is available in "png" format from:

<http://arXiv.org/ps/astro-ph/9408099v1>

This figure "fig2-3.png" is available in "png" format from:

<http://arXiv.org/ps/astro-ph/9408099v1>

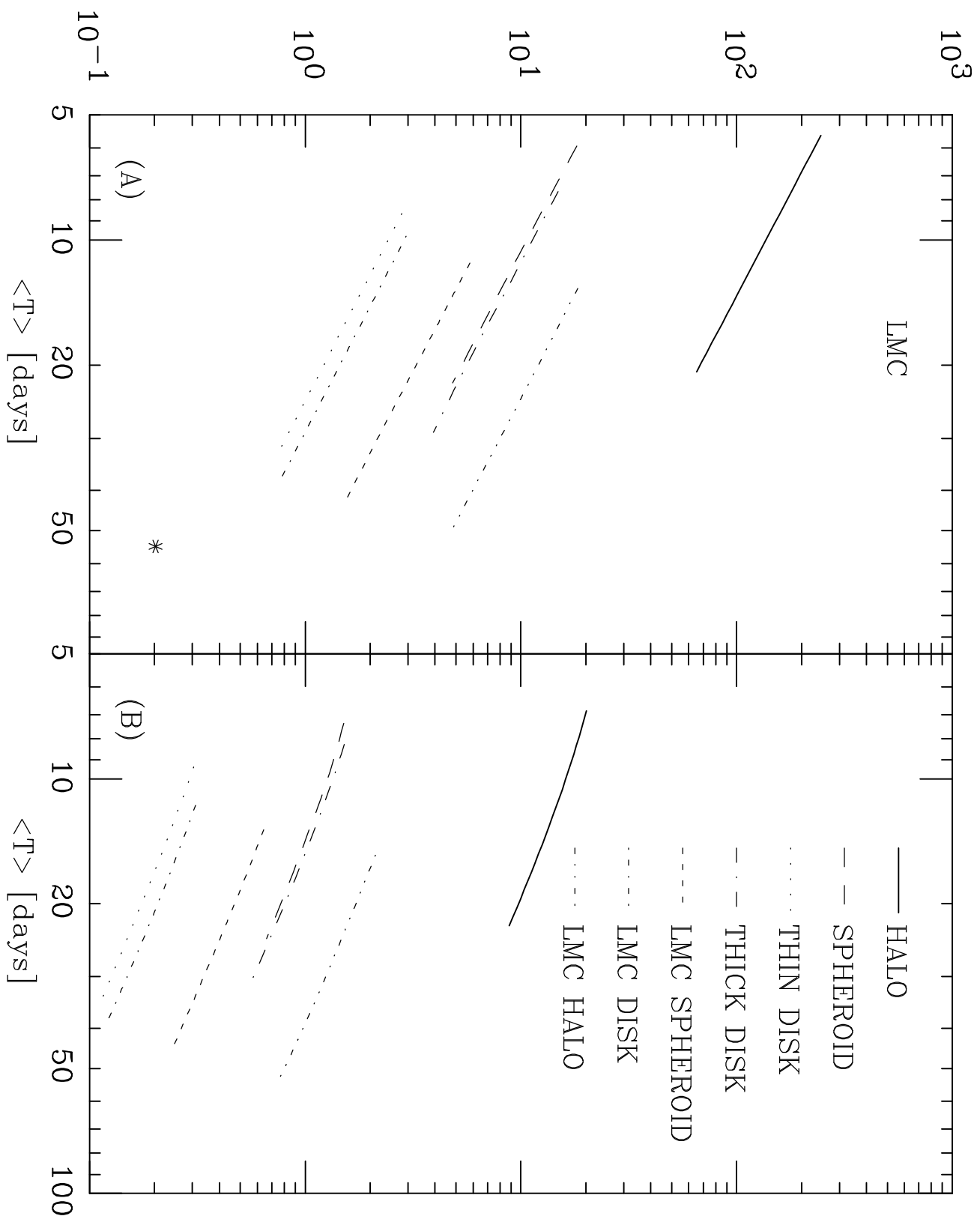
$d\Gamma/dT$  [events/( $10^6$  stars yr day)]



This figure "fig1-4.png" is available in "png" format from:

<http://arXiv.org/ps/astro-ph/9408099v1>

$\Gamma$  [events/( $10^7$  stars yr)]



This figure "fig1-5.png" is available in "png" format from:

<http://arXiv.org/ps/astro-ph/9408099v1>

$\Gamma$  [events/( $10^6$  stars yr)]

